Published in final edited form as:
Biochem Biophys Res Commun. 2005 July 8; 332(3): 670–676. doi:10.1016/j.bbrc.2005.05.006.

Putative tumor suppressor RASSF1 interactive protein and cell death inducer C19ORF5 is a DNA binding protein

Leyuan Liu[a], **Amy Vo**[a], **Guoqin Liu**[a], and **Wallace L. McKeehan**[a,b,*]

[a]Center for Cancer Biology and Nutrition, Institute of Biosciences and Technology, Texas A&M University System Health Science Center, Houston, TX 77030-3303, USA

[b]Department of Biochemistry and Biophysics, Texas A&M University, College Station, TX 77843-2128, USA

Abstract

C19ORF5 is a homologue of microtubule-associated protein MAP1B that interacts with natural paclitaxel-like microtubule stabilizer and candidate tumor suppressor RASSF1A. Although normally distributed throughout the cytosol, C19ORF5 specifically associates with microtubules stabilized by paclitaxel or RASSF1A. At sufficiently high concentrations, C19ORF5 causes mitochondrial aggregation and genome destruction (MAGD). The accumulation on hyperstabilized microtubules coupled to MAGD has been proposed to mediate tumor suppression by the taxoid drug family and RASSF1A. Here, we show that the C-terminus of C19ORF5 (C19ORF5C) interacts with mitochondria-associated DNA binding protein, LRPPRC, in liver cells. Like LRPPRC, C19ORF5 also binds DNA with an affinity and specificity sufficient to be of utility in DNA affinity chromatography to purify homogeneous recombinant C19ORF5C from bacterial extracts. Homogeneous C19ORF5 exhibited no intrinsic DNase activity. Deletion mutagenesis indicated that C19ORF5 selectively binds double stranded DNA through its microtubule binding domain. These results suggest C19ORF5 as a DNA binding protein similar to microtubule-associated proteins tau and MAP2.

Keywords

Aneuploidy; Apoptosis; DNA binding; LRPPRC; MAP1B; Microtubule-associated proteins; Mitochondria; Mitotic spindle; Paclitaxel; RASSF1A; VCY2IP1

C19ORF5 is a multifunctional sequence homologue of microtubule-associated protein MAP1B that interacts with the normally mitochondria-associated paclitaxel-like microtubule stabilizer and candidate tumor suppressor RASSF1A [1–5]. Isoform-specific epigenetic silencing of RASSF1A (3p21.3) by promoter-specific CpG-island hypermethylation occurs at high frequency in human tumors [6–8]. While normally distributed throughout the cytosol, C19ORF5 accumulates on hyperstabilized microtubules induced by either paclitaxel or RASSF1A [2–4]. In addition to these functions, when C19ORF5 accumulates in cells, it causes a unique form of cell death characterized by concentration on mitochondria, followed by an intense perinuclear aggregation of mitochondria resulting in gross degradation of genomic DNA within the aggregates. This cell death related process has been described as mitochondrial aggregation and genome destruction (MAGD), and suggested to mediate tumor suppression by the taxoid drug family and RASSF1A in response to catastrophic

*Corresponding author. Fax: +1 713 677 7512. wmckeehan@ibt.tamhsc.edu (W.L. McKeehan)..

hyperstabilization of spindle microtubules during mitosis [3,4]. Structure function analysis has revealed that both the microtubule binding and MAGD activities reside within distinct domains in the C-terminal 192 amino acid residues of C19ORF5. The microtubule binding and hyperstabilization domain is within a basic sequence of less than 100 residues (A867–S945) while the MAGD activity resides further downstream in a distinct 25-residue sequence (F967–A991) [4].

In addition to mitochondria-associated RASSF1 iso-forms, a yeast two-hybrid interaction screen revealed that C19ORF5 potentially interacts with several other mitochondria-associated proteins [1]. One of the interactions was with LRPPRC (leucine-rich PPR-motif containing protein, AAA67549) [1,9], a nucleic acid binding protein [10,11] comprised of modular domains homologous to proteins involved in cytoskeletal dynamics, nucleocytosolic shuttling, and chromosome activity [9]. Here, we confirmed that C19ORF5 interacts with LRPPRC in mammalian cells. Since LRPPRC [10–12] and other microtubule-associated proteins (MAP2 and tau) [13,14] have been reported to interact with DNA and elevation of C19ORF5 caused massive degradation of DNA associated with its MAGD activity, we investigated whether C19ORF5 might also be a DNA binding protein with DNA degradation activity. We show that the C-terminus of C19ORF5 containing the microtubule and MAGD activities binds DNA with sufficient affinity and selectivity to be of utility in affinity purification. C19ORF5 binds specifically double stranded DNA through its microtubule binding domain, but is free of DNase activity.

Materials and methods

Interaction of C19ORF5C and LRPPRC in mammalian cells

For interaction of differentially tagged recombinant products, about 15 μg of pCMV-C3 vector coding for GFP-LRPPRC [1] or GFP was transiently transfected into COS7 cells in 75 cm^2 flasks and cells were harvested in 1 ml Buffer I (PBS with 1 mM PMSF, 2 μg/ml pepstatin, 2 μg/ml leu-peptin, 10 μg/ml aprotinin, 1 mM EDTA, and 0.1 mM DTT) after 24 h. Cell free extract was prepared by 10 s of sonication followed by 10 min of centrifugation at 10,000g at 4 °C, and then used immediately for assay or stored at −80 °C. About 20 μg of GST-C19ORF5, GST or other GST-tagged control proteins bound to similar amounts of GSH–Sepharose 4B beads was mixed with 200 μl cell free extract and incubated at 4 °C for 2 h after which beads were collected and washed three times with Buffer I. Beads were extracted with 50 μl of gel loading buffer containing SDS, subjected to 7.5% SDS–PAGE, and then analyzed by immunoblot with a polyclonal antibody against GFP.

The interaction of native C19ORF5 and LRPPRC was assessed by immunoprecipitation and subsequent immunoblot using respective monoclonal antibodies against the human proteins. About 1×10^6 HepG2 cells were lysed in 250 μl of immunoprecipitation buffer (IP buffer) containing 50 mM Hepes (pH 7.5), 150 mM NaCl, 1 mM EDTA, 2.5 mM EGTA, 0.1% Triton X-100, 10% glycerol, 1 mM NaF, 1 mM PMSF, 2 μg/ml pepstatin, and 2 μg/ml aprotinin. C19ORF5 protein was precipitated with 9 μg of purified mouse monoclonal antibody 4G1 and 50 μl of packed volume of protein G–agarose beads. A quarter of the precipitate that was resuspended in 100 μl buffer (corresponding to 2.5×10^5 cells) was subjected to immunoblot. Proteins were visualized with 1 μg/ml of 4G1 or monoclonal antibody 4C12 against LRPPRC and 0.1 μg/ml of alkaline phosphatase-conjugated anti-mouse antibody. Monoclonal anti-C19ORF5 antibody 4G1 was generated in collaboration with A&G Pharmaceuticals (Baltimore, MD) using purified GST-C19ORF5C as antigen. The authenticity of the antibody was confirmed by immunoblot of the purified GST-C19ORF5C and other GST fused fragments and immunostain of GFP-C19ORF5C transfected COS7 cells [4]. The epitope has been mapped to within D667–S767 as shown in Fig. 5C. The reactive epitope for the mouse monoclonal anti-LRPPRC antibody Mab4C12

(a gift from Dr. Pinol-Roma, Mount Sinai School of Medicine, New York) was mapped to a sequence between amino acid residues 500 and 600 of LRPPRC by immunoprecipitation of deletion constructs synthesized by in vitro transcription–translation and by immunoblots of constructs expressed in *Escherichia coli* [1,10,15].

Expression and purification of recombinant GST-tagged C19ORF5C and subdomains

DNA coding for GST at the N-terminus of the C-terminal 393 amino acid residues of the predicted full-length 1059 residue C19ORF5 was constructed. The 1.25 kb cDNA C19ORF5-pACT2 [9] was digested with *NcoI* and *Bgl*II, filled into blunt ends, and then ligated into a 5 kb pGEX-4T-1 vector (Pharmacia Biotech) coding for GST after a cut with *Sma*I. The GST-C19ORF5 protein was expressed in *E. coli* BL21 cells harvested in Buffer I containing 0.5 mg/ml lysozyme and purified by glutathione (GSH) affinity according to manufacturer's recommendations. After dialysis in Buffer II (50 mM Tris-HCl, pH 8.0), the solution was then applied to DNA–agarose beads (Amersham-Pharmacia Biotech) at 4 °C overnight. Beads were collected, washed three times with Buffer II, and eluted with 0.5 M NaCl in Buffer II. The eluate was dialyzed against Buffer II. Steps were repeated to achieve homogeneity. Purity of product was assessed by SDS–PAGE. Purified product was subjected to fragmentation and loss of activity upon storage at −4 °C or dilution and was stored concentrated where possible in aliquots at −80 °C until immediate use in in vitro assays.

The cDNA constructs coding for different sections of C19ORF5 fused to the C-terminus of GST as described in the text were constructed through the ligation of the *EcoRI–Not*I cut 5 kb pGEX-4T-1 vector and PCR fragments were generated from template C19ORF5-pACT2 that carried the entire 393 amino acid residues of the C-terminal part of C19ORF5 [9]. Fidelity of constructs was verified by DNA sequence. Constructs were expressed in bacteria and purified by GSH and DNA affinity chromatography as described in the text.

DNA binding and nuclease assays

The DNA aggregation and nuclease assays were developed based on previous reports [16–19]. Aggregation reactions (20 μl) contained identical amounts of DNA (10 μg/ml) and different amounts of purified GST-C19ORF5 protein in 50 mM Tris (pH 8.0), and were incubated at 37 °C for 1 h and stopped by adding 5 μl DNA loading buffer. DNA substrates used were supercoiled double stranded plasmid DNA prepared from the 3.0 kb plasmid pBluescript SK using a Plasmid Midi Kit (Qiagen), *EcoRI* linearized pBluescript SK plasmid DNA, genomic DNA isolated from cultured HepG2 cells, and the ϕX174 virion single stranded DNA purchased from New England Biolabs. DNA was separated on 0.7% agarose gel in 1× TBE buffer. For nuclease assays, 10 μg/ml of the unlabeled pBluescript SK cut with *EcoRI* was incubated with 1 mg/ml GST-C19ORF5 or GST protein at 37 °C for 3 h and resolved on 1.5% agarose gel. The ^{32}P-labeled linear pBluescript SK (125 ng/ml in 10 μl) prepared using the RadPrime DNA Labelling System from Gibco-BRL was incubated with 1 mg/ml GST-C19ORF5 or GST protein at 37 °C for 3 h. The reaction mixture was added with 40 μg of herring carrier DNA, adjusted to 200 μl, and precipitated with 200 μl ice-cold 15% TCA. The acid-soluble radioactivity was quantified by scintillation counting as a measure of DNase activity.

Results

C19ORF5 interacts with nucleic acid binding protein LRPPRC

We confirmed the interaction indicated in a yeast two-hybrid screen with a construct of the 393 C-terminal residues of C19ORF5 tagged at the N-terminus (GST-C19ORF5C) with the nucleic acid binding protein LRPPRC in a mammalian cell context. Extracts of mammalian

cells expressing either recombinant 26 kDa GFP (Fig. 1A, lane 3) or 160 kDa GFP-LRPPRC (Fig. 1A, lane 4) were incubated with purified GST or a construct of the 393 C-terminal residues of C19ORF5 tagged at the N-terminus and then potential complexes were immobilized to GSH–agarose beads. The bead load was examined for capture of 160 kDa GFP-LRPPRC by immunoblot with anti-GFP (lanes 5–8). The immobilized GST-C19ORF5, but not immobilized GST, captured the GFP-LRPPRC as a band of 160 kDa from extracts of GFP-LRPPRC-expressing cells (Fig. 1A, lane 5). Only the non-specific cross-reactive antigen with anti-GFP present in uninfected cells was detected in extracts of cells expressing only GFP (Fig. 1A, lane 7). The interaction of native C19ORF5 and LRPPRC was further confirmed by co-immunoprecipitation from the whole lysates of HepG2 cells with a monoclonal antibody prepared against GST-C19ORF5C (mAb4G1, for epitope see Fig. 5) followed by immunoblot with both mAb4G1 and a monoclonal antibody against LRPPRC (mAb4C12) (Fig. 1B). Analysis of the immunoprecipitates with mAb4G1 revealed that C19ORF5 was present in two major bands, a 113 kDa band that corresponded to full-length (FL) C19ORF5 deduced from cDNA and a short chain (SC) with an apparent mass of 56 kDa. Analysis with mAb4C12 indicated that a single 130 kDa band corresponding to full-length LRPPRC appeared in the C19ORF5 immunoprecipitate.

Affinity of the C19ORF5 C-terminus for DNA and use in affinity purification

To determine whether C19ORF5 was a DNA binding protein similar to its interaction partner LRPPRC, we tested its ability to bind to DNA on immobilized agarose beads. GST-C19ORF5C exhibiting both microtubule and MAGD activities was expressed in bacteria and first subjected to GSH affinity chromatography (Fig. 2). The product obtained by elution with GSH was extremely heterogeneous ranging from the intact fusion product at 68 kDa to GST at about 30 kDa (Fig. 2, lane 4). Extensive washing of the loaded GSH columns with increasing ionic strength up to 2 M NaCl failed to reduce the number of bands. This indicated that bands smaller than the full-length construct were bound tightly but reversibly to the GSH column, carried the GST tag, and thus were likely to be C-terminally truncated products of proteolysis of the N-terminally tagged GST-C19ORF5C. We then tested the interaction of the mixture of GST-tagged products released from the GSH beads with GSH for binding to immobilized DNA. Surprisingly, only the 68 kDa band corresponding to the intact GST-C19ORF5C product bound to and was completely recovered from the DNA affinity matrix (Fig. 2, lanes 5–8). We confirmed that the 68 kDa band extracted by DNA affinity exhibited the GST tag in a second round of GSH affinity purification (Fig. 2, lane 7). The intact GST-C19ORF5C was then purified free of lower molecular weight truncates using multiple rounds of combined glutathione (GSH) and DNA affinity chromatography. These combined steps provided homogeneous GST-C19ORF5C for biochemical studies and monoclonal antibody production, and suggested that C19ORF5 is a DNA binding protein.

C19ORF5C preferentially binds double stranded DNA non-covalently at high protein/DNA ratio

We then examined the interaction of the homogeneous C19ORF5 C-terminus with double stranded supercoiled and linearized DNA in gel mobility shift assays (Fig. 3). GST-C19ORF5C caused an electrophoretic mobility shift to apparent by higher molecular weight of diverse double stranded DNA samples ranging from 3 to 13 kb in agarose gels. The electrophoretic mobility of supercoiled 3.0 kb pBluescript SK plasmid DNA decreased progressively with increasing amounts of purified GST-C19ORF5 (4–30 μM), but not GST alone up to 80 μM (Fig. 3A). Incubation with linearized plasmid DNA resulted in a similar mobility shift (Fig. 3B). In the presence of 0.5 mg/ml (8 μM) GST-C19ORF5, mammalian genomic DNA failed to penetrate the 0.7% agarose gel (Fig. 3C). The shift in mobility was also observed with 5.4 kb single stranded DNA of the ϕX174 virion, but to a much lesser extent than the double stranded substrates (Fig. 3D). This indicated that C19ORF5C

preferentially associates with double stranded DNA. The C19ORF5-induced decrease in mobility of DNA occurred rapidly (Fig. 4A) and at 0 °C(Fig. 4B). The presence of $MgCl_2$ slightly reduced, $MnCl_2$ enhanced, and $CaCl_2$ had no effect on the C19ORF5-dependent decrease in DNA mobility (Fig. 4C). The fact that the mobility shift yielded a broad dispersed band of DNA that was proportional to C19ORF5 concentration with no discrete bands that indicated distinct DNA dimers or higher order oligomers suggested a large binding ratio of C19ORF5 to DNA rather than catalysis of an intermolecular association of DNA through promotion of cohesion or aggregation. No shift in DNA mobility was observed with GST-C19ORF5C after treatment with the non-specific protein cross-linker glutaraldehyde (Fig. 4C, lane GA) [20]. Separate experiments indicated that artificial glutaraldehyde-induced protein aggregates formed a continuum of stained protein bands spanning monomeric GST-C19ORF5 to the sample wells (not shown). This indicated that either DNA is coated with monomeric C19ORF5 or that the cross-linker inactivated the DNA binding activity of C19ORF5. The recovery of control naked DNA from reaction mixtures by standard nucleic acid extraction procedures that remove protein ruled out covalent interaction between DNA molecules catalyzed by C19ORF5 or covalent C19ORF5–DNA complexes (Fig. 4C, lane NP).

Lastly, we extensively tested for an intrinsic DNase activity that might accompany the DNA binding in vitro both by direct incubation and gel analysis as well as testing nucleotide release from radiolabeled double stranded plasmid DNA as described under Materials and methods. Although DNase could be detected in partially purified GST-C19ORF5C preparations relative to GST controls, no activity under a variety of conditions could be detected in the highest purity preparations repurified by GSH affinity after DNA affinity purification. We conclude that the C-terminus of C19ORF5 does not exhibit an intrinsic DNase activity. The residual DNase activity detected in some fractions likely comes from small amounts of bacterial DNases that track with C19ORF5 in less than homogeneous preparations.

The C19ORF5 microtubule binding domain also exhibits the DNA binding

Previously, we mapped the sequence domains for C19ORF5 microtubule binding and MAGD activity, and have shown that they lie within distinct and independent domains in the C-terminus downstream of residue A867 (Fig. 5A). To test whether DNA binding was supported by the same or independent sequence domains, we tested a similar series of constructs tagged with GST for DNA binding. Recombinant products were purified by GST affinity chromatography and then analyzed by SDS–PAGE (Fig. 5B). Immunoblot with monoclonal antibody mAb4G1 prepared against GST-C19ORF5C described earlier in Fig. 1 revealed that the epitope for mAb4G1 was within D667–S766 (Fig. 5C). Analysis of the construct products for DNA binding revealed that neither D667–S766 nor S767–L866 bound to immobilized DNA nor elicited a shift in electrophoretic mobility (Fig. 5D). Construct A867–E966 exhibited both DNA binding activity indicated by binding to DNA affinity columns and the gel shift assay (Fig. 5D). This was despite the fact that the A867–E966 product purified by both GSH and DNA affinity was truncated at the C-terminus by 20–30 residues estimated by apparent molecular weights in the electrophoretic analysis (Fig. 5A). Insolubility of the F967–F1059 product prevented characterization of it in solution. An additional construct S767–E966 that spanned both A767–L866 and A867–E966 confirmed the DNA binding exhibited by A867–E966 (Fig. 5D). These results show that the microtubule binding domain within the C-terminus of C19ORF5 also exhibits DNA binding.

Discussion

In the present study, we demonstrated DNA binding capacity similar to its interaction partner, LRPPRC [10–12], in addition to the other multiple functions of the microtubule-

associated homologue C19ORF5. In this respect, C19ORF5 is similar to two other microtubule-associated proteins, tau and MAP2, whose DNA binding ability has been reported [13,14]. The DNA binding characteristics of C19ORF5 appear most similar to those reported for tau that also exhibited a high protein to DNA binding ratio and a preference for double stranded DNA [21]. Whether C19ORF5 targets specific sequence motifs within DNA as has been reported for LRPPRC [11,12] or MAP2 [13,22,23] requires further study.

Like microtubule-associated proteins tau and MAP2, the role of the DNA binding capacity of C19ORF5 in cellular regulation is unclear. C19ORF5 has recently been implicated in mitochondrial aggregation associated cell death and condensation of genomic DNA followed by massive DNA degradation [3,4]. The high capacity DNA binding suggests a potential direct role in the observed genomic DNA condensation and degradation process. The absence of detectable DNase activity in the homogeneous protein eliminated a direct role in the observed DNA degradation. However, C19ORF5 could play an adaptor role for attraction of mitochondrial and extramitochondrial DNases to the bound DNA similar to the DNA binding activity of mitochondrial-associated apoptosis inducing factor (AIF) that is required for chromatin condensation and large-scale DNA fragmentation during apoptosis [24–26]. It should be noted that the microtubule binding and MAGD activities of C19ORF5 are underpinned by two distinct and independent sequence domains within the last 200 residues of the C-terminus of C19ORF5 [4]. Although we cannot eliminate the possibility of additional DNA binding capacity in the minimal 25 amino acid residue MAGD domain downstream of the microtubule binding sequence (Fig. 5A), our current results suggest that the C19ORF5 DNA binding capacity may lie within the independent microtubule binding domain.

Villasante et al. [27] discussed in detail the possibility that MAP2 and related proteins may play a bridging role between spindle microtubules and the centromeric zone of chromosomes that are enriched in repetitive DNA sequences and the consequences of separate or overlapping microtubule and DNA binding domains. Although conceivably a more detailed mutagenesis might separate the DNA binding and microtubule binding domains within A867-S945, our results indicate that the two activities are likely overlapping. This suggests a potential competition between DNA and microtubules for binding to C19ORF5 rather than a role in bridging DNA and microtubules in a three-way interaction.

Acknowledgments

This work was supported by Public Health Service Grants DK35310 from NIDDK and CA59971 from NCI, National Institutes of Health. We thank Dr. Serafín Piñ-Roma of Mount Sinai School of Medicine (New York) for mouse monoclonal antibody against LRPPRC and Dr. Le Sun and Joe Corvera of A&G Pharmaceutical (Columbia, Maryland) for mouse monoclonal antibody (4G1) against C19ORF5.

References

[1]. Liu L, Vo A, Liu G, McKeehan WL. Novel complex integrating mitochondria and the microtubular cytoskeleton with chromosome remodeling and tumor suppressor RASSF1 deduced by in silico homology analysis, interaction cloning in yeast, and colocalization in cultured cells. In Vitro Cell. Dev. Biol. Anim. 2002; 38:582–594. [PubMed: 12762840]

[2]. Dallol A, Agathanggelou A, Fenton SL, Ahmed-Choudhury J, Hesson L, Vos MD, Clark GJ, Downward J, Maher ER, Latif F. RASSF1A interacts with microtubule-associated proteins and modulates microtubule dynamics. Cancer Res. 2004; 64:4112–4116. [PubMed: 15205320]

[3]. Liu L, Vo A, McKeehan WL. Specificity of the methylation-suppressed A isoform of candidate tumor suppressor RASSF1 for microtubule hyperstabilization is determined by cell death inducer C19ORF5. Cancer Res. 2005; 65:1830–1838. [PubMed: 15753381]

[4]. Liu L, Vo A, Liu G, McKeehan WL. Distinct structural domains within C19ORF5 support association with stabilized microtubules and mitochondrial aggregation and genome destruction. Cancer Res. 2005; 65:4191–4201. [PubMed: 15899810]

[5]. Song MS, Chang JS, Song SJ, Yang TH, Lee H, Lim DS. The centrosomal protein RABP1 regulates mitotic progression by recruiting RASSF1A to spindle poles. J. Biol. Chem. 2005; 280:3920–3927. [PubMed: 15546880]

[6]. Burbee DG, Forgacs E, Zochbauer-Muller S, Shivakumar L, Fong K, Gao B, Randle D, Kondo M, Virmani A, Bader S, Sekido Y, Latif F, Milchgrub S, Toyooka S, Gazdar AF, Lerman MI, Zabarovsky E, White M, Minna JD. Epigenetic inactivation of RASSF1A in lung and breast cancers and malignant phenotype suppression. J. Natl. Cancer Inst. 2001; 93:691–699. [PubMed: 11333291]

[7]. Dammann R, Li C, Yoon JH, Chin PL, Bates S, Pfeifer GP. Epigenetic inactivation of a RAS association domain family protein from the lung tumour suppressor locus 3p21.3. Nat. Genet. 2000; 25:315–319. [PubMed: 10888881]

[8]. Dammann R, Schagdarsurengin U, Seidel C, Strunnikova M, Rastetter M, Baier K, Pfeifer GP. The tumor suppressor RASSF1A in human carcinogenesis: an update. Histol. Histopathol. 2005; 20:645–663. [PubMed: 15736067]

[9]. Liu L, McKeehan WL. Sequence analysis of LRPPRC and its SEC1 domain interaction partners suggest roles in cytoskeletal organization, vesicular traicking, nucleocytosolic shuttling and chromosome activity. Genomics 79. 2002:124–136.

[10]. Mili S, Pinol-Roma S. LRP130, a pentatricopeptide motif protein with a noncanonical RNA-binding domain, is bound in vivo to mitochondrial and nuclear RNAs. Mol. Cell. Biol. 2003; 23:4972–4982. [PubMed: 12832482]

[11]. Tsuchiya N, Fukuda H, Sugimura T, Nagao M, Nakagama H. LRP130, a protein containing nine pentatricopeptide repeat motifs, interacts with a single-stranded cytosine-rich sequence of mouse hypervariable minisatellite Pc-1. Eur. J. Biochem. 2002; 269:2927–2933. [PubMed: 12071956]

[12]. Labialle S, Dayan G, Gayet L, Rigal D, Gambrelle J, Baggetto LG. New invMED1 element *cis*-activates human multidrug-related MDR1 and MVP genes, involving the LRP130 protein. Nucleic Acids Res. 2004; 32:3864–3876. [PubMed: 15272088]

[13]. Avila J, Montejo de Garcini E, Wandosell F, Villasante A, Sogo JM, Villanueva N. Microtubule-associated protein MAP2 preferentially binds to a dA/dT sequence present in mouse satellite DNA. EMBO J. 1983; 2:1229–1234. [PubMed: 10872313]

[14]. Schroder HC, Bernd A, Zahn RK, Muller WE. Binding of polyribonucleotides and polydeoxyribonucleotides to bovine brain microtubule protein: age-dependent modulation via phosphorylation of high-molecular-weight microtubule-associated proteins and tau proteins. Mech. Ageing Dev. 1984; 24:101–117. [PubMed: 6141331]

[15]. Mili S, Shu HJ, Zhao Y, Pinol-Roma S. Distinct RNP complexes of shuttling hnRNP proteins with pre-mRNA and mRNA: candidate intermediates in formation and export of mRNA. Mol. Cell. Biol. 2001; 21:7307–7319. [PubMed: 11585913]

[16]. Baumann P, Benson FE, West SC. Human Rad51 protein promotes ATP-dependent homologous pairing and strand transfer reactions in vitro. Cell. 1996; 87:757–766. [PubMed: 8929543]

[17]. Losada A, Hirano T. Intermolecular DNA interactions stimulated by the cohesin complex in vitro: implications for sister chromatid cohesion. Curr. Biol. 2001; 11:268–272. [PubMed: 11250156]

[18]. Widlak P, Li P, Wang X, Garrard WT. Cleavage preferences of the apoptotic endonuclease DFF40 (caspase-activated DNase or nuclease) on naked DNA and chromatin substrates. J. Biol. Chem. 2000; 275:8226–8232. [PubMed: 10713148]

[19]. Widlak P, Li LY, Wang X, Garrard WT. Action of recombinant human apoptotic endonuclease G on naked DNA and chromatin substrates: cooperation with exonuclease and DNase I. J. Biol. Chem. 2001; 276:48404–48409. [PubMed: 11606588]

[20]. Jayakrishnan A, Jameela S. Glutaraldehyde as a fixative in bioprostheses and drug delivery matrices. Biomaterials. 1996; 17:471–484. [PubMed: 8991478]

[21]. Hua Q, He RQ, Haque N, Qu MH, del Carmen Alonso A, Grundke-Iqbal I, Iqbal K. Microtubule associated protein tau binds to double-stranded but not single-stranded DNA. Cell. Mol. Life Sci. 2003; 60:413–421. [PubMed: 12678504]

[22]. Marx KA, Denial T, Keller T. High-affinity microtubule protein-higher organism DNA complexes. Many-fold enrichment in repetitive mouse DNA sequences comprised of satellite DNAs. Biochim. Biophys. Acta. 1984; 783:283–292. [PubMed: 6391551]

[23]. Marx KA, Denial T. High affinity DNA-microtubule interactions: evidence for a conserved DNA-MAP interaction involving unusual high CsCl density repetitious DNA families. Mol. Cell. Biochem. 1992; 118:39–48. [PubMed: 1488054]

[24]. Lipton SA, Bossy-Wetzel E. Dueling activities of AIF in cell death versus survival: DNA binding and redox activity. Cell. 2002; 111:147–150. [PubMed: 12408857]

[25]. Susin SA, Lorenzo HK, Zamzami N, Marzo I, Snow BE, Brothers GM, Mangion J, Jacotot E, Costantini P, Loeffler M, Larochette N, Goodlett DR, Aebersold R, Siderovski DP, Penninger JM, Kroemer G. Molecular characterization of mitochondrial apoptosis-inducing factor. Nature. 1999; 397:441–446. [PubMed: 9989411]

[26]. Ye H, Cande C, Stephanou NC, Jiang S, Gurbuxani S, Larochette N, Daugas E, Garrido C, Kroemer G, Wu H. DNA binding is required for the apoptogenic action of apoptosis inducing factor. Nat. Struct. Biol. 2002; 9:680–684. [PubMed: 12198487]

[27]. Villasante A, Corces VG, Manso-Martinez R, Avila J. Binding of microtubule protein to DNA and chromatin: possibility of simultaneous linkage of microtubule to nucleic and assembly of the microtubule structure. Nucleic Acids Res. 1981; 9:895–908. [PubMed: 7232207]

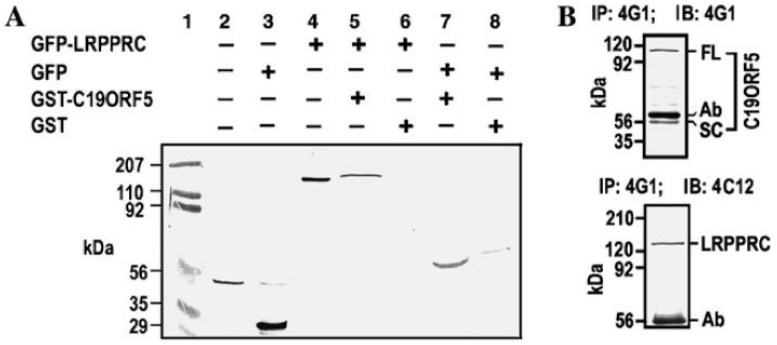

Fig. 1.

Interaction of C19ORF5 with DNA binding protein LRPPRC. (A) Interaction of recombinant C19ORF5 and LRPPRC in mammalian extracts. GFP-LRPPRC [1] from cell extracts was captured by purified GST-C19ORF5 immobilized on GSH beads and then visualized by immunoblot with anti-GFP antibody in assays described under Materials and methods. Cells were transfected with GFP-LRPPRC or GFP alone as indicated, extracts containing about 200 μg of total protein were loaded directly (lanes 2–4), or incubated with beads loaded with 20 lg of purified GST-C19ORF5 or GST prior to analysis as indicated (lanes 5–8). Content of the agarose beads was analyzed in lanes 5–8. Lane 1, protein standards. (B) Co-immunoprecipitation of native LRPPRC and C19ORF5 from HepG2 cells. C19ORF5 was immunoprecipitated (IP) with anti-C19ORF5 (monoclonal 4G1) from lysates of HepG2 cells and then analyzed on immunoblot (IB) with 4G1 or anti-LRPPRC (monoclonal 4C12). The indicated blots represent the lysate from 2.5×10^5 cells. FL, full-length C19ORF5 predicted by translation; SC, 56 kDa short chain of C19ORF5; and Ab, mouse IgG heavy chain.

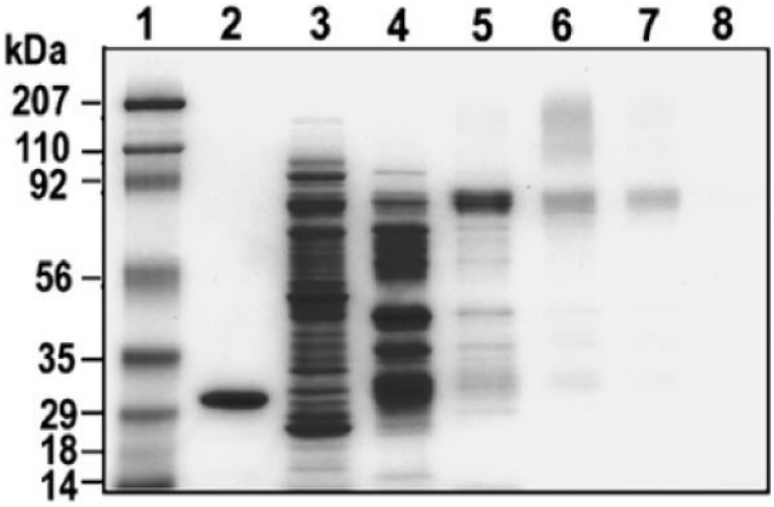

Fig. 2.

Purification of GST-C19ORF5C to homogeneity by combined GSH and DNA affinity chromatography. GST-C19ORF5 (residues 667–1059) was expressed in bacteria, extracted, and subjected to affinity chromatography on GSH or DNA immobilized to agarose beads as described under Materials and methods. Fractions were analyzed by SDS–PAGE and the protein was visualized by Coomassie blue stain. Lane 1, protein standards with the indicated apparent molecular mass; lane 2, GSH eluate from GSH beads of extract from bacteria expressing only the fusion tag GST; lane 3, whole extract of cells expressing GST-C19ORF5; lane 4, GSH eluate of the extract in lane 3 from GSH beads; lane 5, GSH eluate of the extract from lane 4 captured on DNA–agarose beads; lane 6, 0.5 M NaCl eluate from DNA–agarose beads; lane 7, repurification of the eluate from lane 6 on GSH beads; and lane 8, residual DNA–agarose beads from lane 6 after the 0.50 M NaCl elution. About 10 μg protein was applied to lane 3.

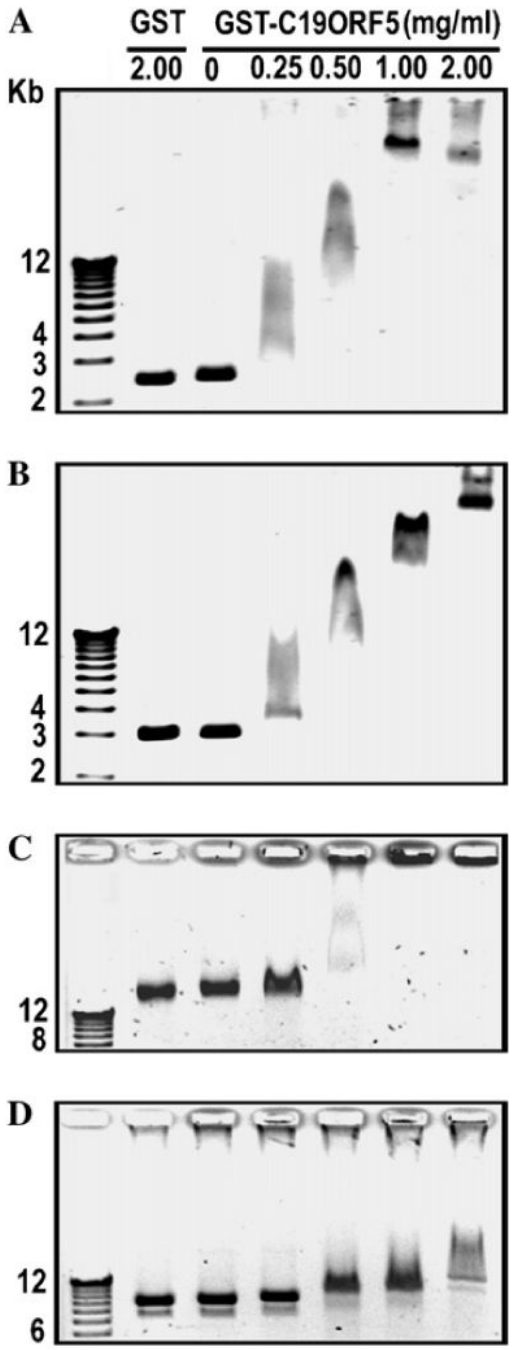

Fig. 3.

Interaction of purified GST-C19ORF5C with different types of DNA. (A) Double stranded, supercoiled pBluescript SK plasmid, (B) double stranded *BamHI* linearized pBluescript SK, (C) double stranded HepG2 genomic DNA (10 μg/ml), and (D) single strand ϕ X174 virion DNA were incubated with the indicated amounts of homogeneous GST-C19ORF5 or GST for 1 h at 37 °C.

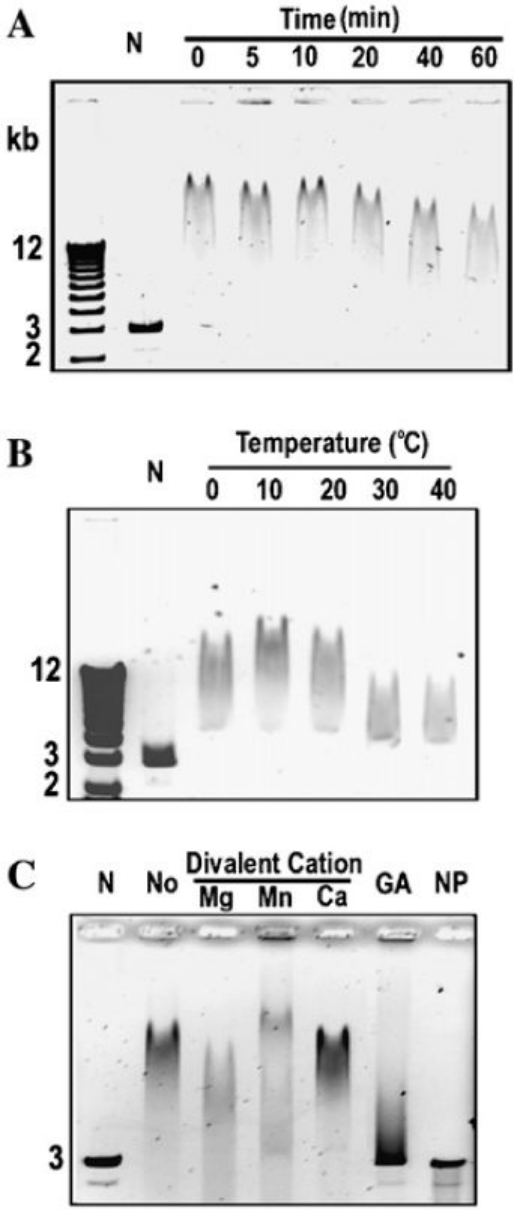

Fig. 4.

Influence of time, temperature, divalent cations, and protein cross-linking on association of purified GST-C19ORF5C with DNA. (A) Linearized pBluescript SK plasmid (10 μg/ml) was incubated with GST-C19ORF5 (2 mg/ml) for the indicated times at 37 °C or (B) the indicated temperature for 1 h. N, no GST-C19ORF5 added. (C) Effect of divalent cations (10 mM) and glutaraldehyde-induced protein cross-linking (GA) on DNA mobility. Assays contained 10 μg/ml of linearized pBluescript SK, 2 mg/ml GST-C19ORF5 protein for 1 h at 37 °C. No, GST-C19ORF5 with no divalent cations added; NP, a reaction mixture depleted of protein with the QLAquick PCR purification kit for extraction of DNA.

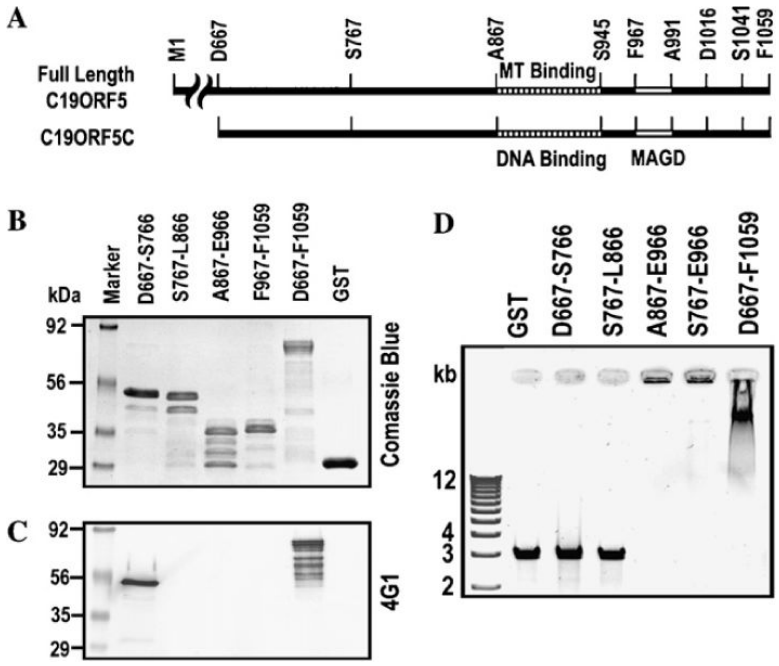

Fig. 5.

Identification of the DNA binding domain of C19ORF5. (A) Sequence domain structure of C19ORF5. Full-length C19ORF5 and the 393 amino acid residue C19ORF5C (D667–F1059) with residues flanking constructs utilized in this study are indicated. Assignment of the minimum DNA and microtubule binding domain is based on an estimate of the minimum length of a truncated product of GST-A867–E966 that bound microtubules and DNA, and homology with the microtubule binding domain of MAP1A and MAP1B [4]. F967–A991 is the MAGD domain. (B) Recombinant GST-tagged C19ORF5 subdomains expressed in bacteria. GST, D667–S766, and S767–L866 were purified by GSH affinity. A867–E966, S767–E966, and D667–F1059 were purified by both GSH and DNA affinity. Insoluble F967–F1059 was extracted directly from cells with SDS buffer. Each lane was loaded with about 10 μg protein that was visualized with Coomassie blue. (C) Specificity of monoclonal antibody 4G1. About 40 μg of the indicated expression products was analyzed by SDS–PAGE and stained with Coomassie blue. About 400 ng was subjected to immunoblot with monoclonal antibody 4G1 as described under Materials and methods. (D) DNA binding of C19ORF4 subdomains indicated by gel shift assay. The indicated purified expression products (about 2 mg/ml) were added to 10 μg/ml of 3 kb linear pBluescript SK DNA and incubated for 1 h at 37 °C prior to analysis.